

## Resonant inelastic x-ray scattering of spin-charge excitations in a Kondo system

B. Tegomo Chiogo<sup>1</sup>, J. Okamoto<sup>2</sup>, J.-H. Li<sup>2</sup>, T. Ohkochi<sup>3</sup>, H.-Y. Huang<sup>2</sup>, D.-J. Huang<sup>2</sup>, C.-T. Chen<sup>2</sup>, C.-N. Kuo<sup>4,5</sup>, C.-S. Lue<sup>4,5</sup>, A. Chainani<sup>2</sup> and D. Malterre<sup>1,\*</sup>

<sup>1</sup>*Institut Jean Lamour, Université de Lorraine, CNRS, F-54000 Nancy, France*

<sup>2</sup>*National Synchrotron Radiation Research Center, Hsinchu Science Park, Hsinchu 30076, Taiwan*

<sup>3</sup>*Japan Synchrotron Radiation Research Institute, Sayo-cho, Sayo-gun, Hyogo 679-5198, Japan*

<sup>4</sup>*Department of Physics, National Cheng Kung University, Tainan 70101, Taiwan*

<sup>5</sup>*Taiwan Consortium of Emergent Crystalline Materials, National Science and Technology Council, Taipei 10601, Taiwan*



(Received 16 June 2022; revised 15 August 2022; accepted 15 August 2022; published 24 August 2022)

Resonant inelastic x-ray scattering (RIXS) studies across the Ce  $M_5$  edge have been carried out to investigate the electronic structure of the ferromagnetic CeAgSb<sub>2</sub> Kondo system. The RIXS spectra exhibit energy loss features corresponding to final states usually observed by combining photoemission and inverse photoemission spectroscopy. At low energy loss, a clear signature of the spectral features corresponding to the spin-orbit interaction is also observed. Polarization dependence provides evidence for the  $^1S_0$  symmetry singlet ground state by a total suppression of the  $f^0$  final state. A simplified single-impurity Anderson model combined with full multiplet theory allows an accurate description of the spin-charge excitations. The RIXS data also reveal a strong temperature  $T$  dependence of the fluorescencelike structure. We conjecture that this behavior reflects the  $T$  dependence of the Kondo resonance.

DOI: [10.1103/PhysRevB.106.075141](https://doi.org/10.1103/PhysRevB.106.075141)

### I. INTRODUCTION

Cerium compounds exhibit very interesting electronic and magnetic properties such as the Kondo effect, intermediate valence, heavy-fermion behavior, and unconventional superconductivity (for a review see [1,2] and references therein). These properties are due to the strongly localized  $4f$  electrons and their hybridization with conduction band states. Theoretically, the complete physics of  $f$ -electron systems is in the periodic Anderson model. While a precise understanding of electronic properties of Kondo systems requires a knowledge of both the low- and high-energy scales, the main aspects of the spectroscopic properties are satisfactorily described by the single-impurity Anderson model (SIAM). The SIAM contains the high-energy scales (the energy of the localized  $f$  states  $\epsilon_f$ , the on-site Coulomb interaction  $U_{ff}$ , and the hybridization strength  $\Delta$ ) and also an emergent low-energy scale (the Kondo energy  $k_B T_K$ ) [3].

In the last few decades, the Kondo scenario for Ce compounds has been extensively investigated by combining the SIAM with high-energy electron spectroscopies such as core-level and valence band photoemission spectroscopy (PES) [4–11], inverse PES (IPES) [12–17], x-ray absorption spectroscopy (XAS) [4,18], and resonant IPES (RIPES) [19,20]. The SIAM utilizes  $f^0$ ,  $f^1$ , and  $f^2$  configurations with spin-orbit interaction lifting the degeneracy of the  $4f$  orbital to  $J = 5/2$  and  $J = 7/2$  for describing Ce-based systems. Hybridization between the  $4f$  states and the conduction band states results in lifting the  $f^1_{5/2}$  degeneracy and stabilizes a singlet Kondo state. This singlet state is a hybrid of the different configurations and lower in energy than the first excited

magnetic states by the Kondo energy  $k_B T_K$ . The singlet ground state is expressed as

$$|G\rangle = a|f^0\rangle + b|f^1_{5/2}\underline{L}\rangle + c|f^1_{7/2}\underline{L}\rangle + d|f^2\underline{L}^2\rangle,$$

where  $\underline{L}$  denotes a hole in the conduction band. Similarly, the degeneracy of the  $f^1_{7/2}$  spin-orbit level is also lifted, and a singlet state which resembles the Kondo ground state is also formed and located at  $k_B T_K + \Delta_{so} - k_B T_{ex}$ , where  $k_B T_{ex}$  stands for the energy gain of the singlet formed from the  $J = 7/2$  manifold [3]. While thermodynamic techniques yield access to the low-energy scales (Kondo and crystal-field energies), including coherence, it misses the high-energy scales. On the other hand, electron spectroscopies in combination with SIAM, while missing coherence properties, have, nonetheless, established their role for precise understanding of high-energy spectroscopy and Kondo energy scale properties. However, the strong surface sensitivity of electron spectroscopy remains an issue and makes RIXS important.

RIXS is a photon in/photon out technique able to directly probe elementary excitations especially in strongly correlated systems like Ce compounds [21,22]. The advantages of RIXS spectroscopy are (i) its bulk sensitivity and (ii) its resonant character, which allows us to enhance the  $4f$  signal. For example, the Ce  $M_{4,5}$  spectral feature associated with the  $f^0$  contribution in the ground state has a very small spectral weight in low- $T_K$  compounds, whereas the corresponding feature in RIXS spectra exhibits a sizable intensity. Moreover, the initial and final states in RIXS are not governed by dipole selection rules, so intrashell  $f$ - $f$  transitions like spin-orbit, crystal-field, and  $f^1 \rightarrow f^2$  or  $f^1 \rightarrow f^0$  excitations are allowed. It was theoretically predicted by Kotani [23] that RIXS spectroscopy can also probe the Kondo resonance in Ce compounds.

\*Corresponding author: daniel.malterre@univ-lorraine.fr

Early measurements by Butorin *et al.* on an  $f^0$  system (CeO<sub>2</sub>) at the Ce  $M_{4,5}$  edge showed that RIXS is an efficient way to determine charge excitations [24–26]. Magnuson *et al.* [27] measured Ce  $M_{4,5}$  and  $N_{4,5}$  RIXS of the Kondo material CeB<sub>6</sub> and determined the  $f^1 \rightarrow f^2$  charge excitation energies. Dallera *et al.* then showed that polarization-dependent RIXS is very useful for determining the degree of hybridization between the localized and extended states on the well-known  $\alpha$ -Ce and  $\gamma$ -Ce compounds [28]. More recently, the development of high-resolution soft x-ray RIXS spectroscopy allowed Amorese *et al.* to precisely access low-energy crystal-field and spin-orbit excitations in Ce compounds [29–32].

In this paper, we report the results of a RIXS study on the CeAgSb<sub>2</sub> Kondo compound. CeAgSb<sub>2</sub> is a weakly hybridized compound with a low Kondo temperature estimated to be  $T_K \sim 65$  K from susceptibility [33] and to be  $\sim 60$ – $80$  K from inelastic neutron scattering [34] as well as muon spin rotation measurements [35]. However, a value of  $T_K \sim 23$  K was also proposed from an analysis based on the relation between the Kondo temperature and the Wilson number [33]. While the competition between the Ruderman-Kittel-Kasuya-Yosida (RKKY) interaction and the Kondo effect usually results in an antiferromagnetic ground state when the RKKY interaction is stronger than the Kondo effect, CeAgSb<sub>2</sub> exhibits an unusual ferromagnetic ordering at  $T_C = 9.8$  K [36]. In such ferromagnetic Kondo lattices, the Kondo temperature is very close to  $T_C$ , usually just above it [37]. Therefore, in CeAgSb<sub>2</sub>, we can conclude that  $T_K$  is likely in the 10–20 K range. The weakly intermediate valence character was revealed by high-resolution valence band PES, XAS at the  $M_{4,5}$  [38] edge, and, more recently, Ce  $4d$ - $4f$  resonant PES measurements [39].

We investigate the  $f^1 \rightarrow f^0$  and  $f^1 \rightarrow f^2$  charge excitations and also  $f^1 \rightarrow f^1$  transitions close to the elastic peak (Kondo resonance and spin-orbit satellite) in CeAgSb<sub>2</sub> using Ce  $M_5$  edge RIXS. We simulate the spectra with calculations based on the SIAM with a zero bandwidth of the conduction band [40], combined with the full multiplet theory, by using the QUANTY code [41,42]. We also study the drastic polarization dependence of the  $f^0$  structure and the RIXS quasielastic peak, which yields access to the symmetry of the ground state [23,43]. Interestingly, we observe  $T$  dependence of the fluorescence-like structure, which has not been reported to date for any Kondo system, and we propose that this  $T$  dependence reflects Kondo behavior.

## II. EXPERIMENTAL DETAILS

We performed Ce  $M_5$  edge RIXS measurements of CeAgSb<sub>2</sub> with the AGM-AGS spectrometer [44] at beamline 05A of the Taiwan Light Source of the National Synchrotron Radiation Research Center, Taiwan. The scattering geometry of the RIXS measurement is illustrated in Fig. S1 in the Supplemental Material (SM) [45]. The surface of the single-crystalline CeAgSb<sub>2</sub> sample was a naturally cleaved  $ab$  plane. The incident angle  $\theta$  and the scattering angle  $\phi$  were  $20^\circ$  and  $90^\circ$ , respectively. The RIXS spectra were recorded with the polarization of the incident x ray that was switchable between  $\sigma$  and  $\pi$  polarizations, i.e., the electric field vector of the linearly polarized light perpendicular to and within the scattering

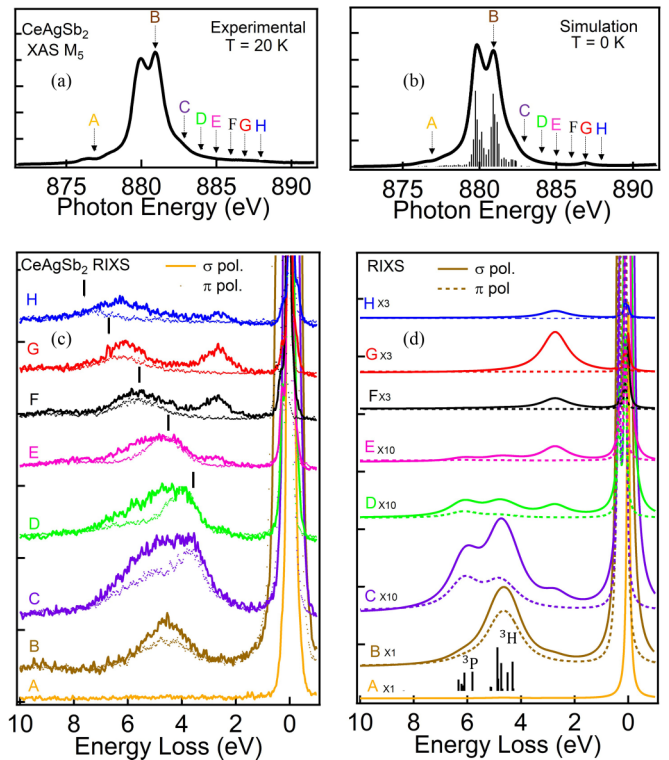


FIG. 1. (a) Experimental Ce  $3d_{5/2}$  x-ray absorption spectra of CeAgSb<sub>2</sub> at 20 K. (b) Calculated XAS spectrum at the Ce  $M_5$  edge at  $T = 0$  K. (c) A set of RIXS spectra for different  $h\nu$  values at 300 K with  $\sigma$  and  $\pi$  polarization. (d) Calculated RIXS spectra with  $\sigma$  and  $\pi$  polarization at  $T = 0$  K.

plane, respectively, and the polarization of the scattered x rays was not analyzed. The total energy resolution of RIXS was 120 meV. The total energy resolution and calibration of the energy loss were estimated by the elastic scattering peak of the RIXS spectra of carbon tape, which were measured before and after the RIXS measurement of CeAgSb<sub>2</sub> with  $\sigma$  polarization. The base pressure of the RIXS chamber was  $\sim 10^{-8}$ . RIXS spectra were recorded at temperatures from 20 K to room temperature; the sample was cooled down with liquid helium.

The incident photon energies were determined by the Ce  $M_5$  edge XAS measurement of CeAgSb<sub>2</sub> with the total-fluorescence-yield method; the incident angle  $\theta$  was set to  $40^\circ$ , and the fluorescence signal was detected by the photodiode set at a scattering angle  $\phi$  of  $115^\circ$ . The energy resolution of XAS was  $\sim 0.3$  eV. In our simulations, we describe the ground state and the XAS and RIXS spectra in the framework of the single-impurity Anderson model by neglecting the fact that the ground state is ferromagnetic, and we focus on the Kondo ground state. This is justified by the fact that all measurements reported here were carried out for  $T > T_C$ . The simulation details are given in Sec. B of the SM.

## III. RESULTS AND DISCUSSION

Figure 1(a) shows the Ce  $3d_{5/2}$  XAS spectrum at  $T = 20$  K. It exhibits a structured feature around  $E = 881$  eV corresponding mainly to the well-known  $3d_{5/2}^9 f^2$  multiplet states due to the strong interaction between the  $3d_{5/2}$  core hole

and the Ce  $4f$  states [18]. There is also a very weak satellite at  $E = 887$  eV which corresponds to the  $3d^9_{5/2}f^1$  final states. The intensity of this satellite in XAS spectra reflects the  $f^0$  contribution in the ground state [18,46]. Figure 1(c) shows a set of RIXS spectra of CeAgSb<sub>2</sub> recorded at  $T = 300$  K for several incident photon energy  $h\nu$  values labeled A to H in the XAS spectrum [Fig. 1(a)] across the Ce  $M_5$  edge. Two different geometries are used for linearly polarized incident x rays with the scattering angle fixed to  $90^\circ$  (see Fig. S1 in the SM): (i) a polarized geometry, for which the incident x ray is perpendicular to the scattering plane ( $\sigma$  polarization), and (ii) a depolarized geometry, for which the incident x ray is parallel to the scattering plane ( $\pi$  polarization). When the incident  $h\nu$  is tuned on the main peak of the XAS (point B), the RIXS spectrum for both polarizations exhibits two features: the quasielastic peak at nearly zero energy loss and a broad structure at 4.5 eV loss energy which shows some variation in peak shape and width on increasing  $h\nu$ . When  $h\nu$  is tuned at the weak satellite (point G), an additional inelastic structure is observed at 2.7 eV energy loss in the  $\sigma$  polarization. The RIXS spectra exhibit a strong polarization dependence; namely, the 2.7 eV structure is completely suppressed, and the broad feature in the 3–7 eV range is reduced in  $\pi$  polarization. Moreover, an additional inelastic scattering peak (indicated by the vertical bars) corresponding to a constant scattering photon energy is also observed and is therefore a clear signature of a fluorescence signal and will be discussed below. By comparing RIXS data with PES and IPES spectra results [12–17,38,39], the quasielastic peak is assigned to  $f^1$  final states, the 2.7 eV feature is the  $f^0$  final state, and the 3–7 eV feature is the  $f^2$  multiplet final states. Thus, all the charge excitations observed in combined PES/IPES experiments can be evidenced in RIXS.

In order to firmly establish the assignments, we calculated the XAS and RIXS spectra [Figs. 1(b) and 1(d)] using a simplified Anderson impurity model combined with full multiplet configuration-interaction calculations [47] using the QUANTY code [41,42] (see the SM for calculation details). The calculated RIXS results are compared with  $T = 300$  K experimental spectra, which is legitimated by the fact that the experimental energy loss features are essentially  $T$  independent (see Fig. S3 in the SM). The XAS and RIXS spectra calculated for the same set of electronic parameters correspond to an intermediate valence ground state ( $n_f = 0.987$ ) and are in good agreement with the experimental spectra shown in Figs. 1(a) and 1(b), except for the fluorescencelike feature, which is not included in the model. While the  $f^0$  final state consists of a single peak with no multiplets and is resonantly enhanced at the weak XAS satellite feature (point G), the  $f^2$  states show clear multiplet effects due to strong  $4f$ - $4f$  interactions. Indeed, when  $h\nu$  is tuned on point B, the  $f^2$  final states mainly consist of the  $^3H$  multiplets. On increasing  $h\nu$  from point B to C, the  $f^2$  states evolve into two sets of multiplets consisting mainly of the  $^3H$  and  $^3P$  multiplets. Similar multiplet effects have been observed on the  $f^2$  final state of RIPES at the Ce  $N_{4,5}$  edge of cerium intermetallic compounds [19]. It should be noted that it is impossible to reproduce the  $f^2$  states in RIXS spectra without taking into account the  $3d^94f^3$  configuration in the intermediate state (the  $f^2$  contribution in the ground state), and this is exemplified

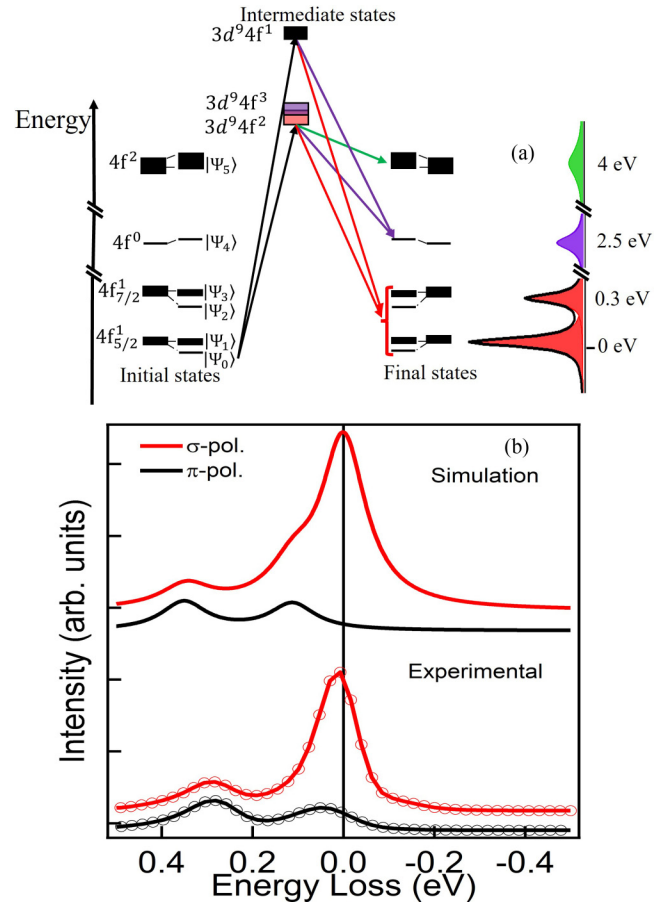


FIG. 2. (a) Total energy level scheme of RIXS of cerium  $M_5$  (initial, intermediate, and final states of the process) and the shape of the RIXS spectrum with the different excitations. In the intermediate state, the red and purple rectangles correspond to the  $3d^94f^3$  and  $3d^94f^2$  configurations, respectively, which overlap. (b) Experimental ( $T = 20$  K) and calculated low energy loss RIXS structures in  $\pi$  and  $\sigma$  polarizations with the incident photon energy tuned on point B.

by the spectral changes seen on increasing  $h\nu$  from point B to C. The  $3d^94f^3$  energies are very close to the  $3d^94f^2$  ones since the negative core-hole- $4f$  Coulomb interactions nearly compensate the additional  $f$ - $f$  Coulomb repulsion in the  $f^3$  configuration [see Fig. 2(a)]. We would like to point out that the spectral weight of the so-called  $f^2$  structure is underestimated in the simulated spectra, especially for high photon energies. Next, we discuss an original characteristic of the RIXS spectra of cerium mixed-valence compounds, namely, the drastic polarization dependence of the  $f^0$  final state and the quasielastic peak. Polarization dependence is very useful to determine the symmetry of the ground state, which is given either by the Kramers doublet due to the crystal-field effect in a purely trivalent system or by  $^1S_0$  symmetry (singlet ground state) for a mixed-valent Ce compound [23]. Nakazawa *et al.* [43] theoretically showed that the polarization dependence of the quasielastic peak and the  $f^0$  features of CeO<sub>2</sub> are strongly dependent on the scattering angle and disappears completely in  $\pi$  polarization with a scattering angle of  $90^\circ$ . This was confirmed experimentally by Watanabe *et al.* [48] and theoretically by Sasabe *et al.* [49]. Indeed, since the ground state must

have the same symmetry as the  $f^0$  state due to hybridization, its total angular momentum  $J$  is zero. Moreover, owing to the experimental geometry ( $90^\circ$  of scattering angle), the x-ray emission (see Fig. S4 in the SM) in the  $z$  direction (which corresponds to an x-ray polarization  $q = 0$ ) is forbidden. Then, following the dipole selection rule in the emission process  $\Delta M = \pm 1$  (where  $M = 0$  is the  $z$  component of the angular momentum of the intermediate states), the  $f^0$  final state and the quasielastic peak are forbidden.

Looking closely at the RIXS spectra in the energy loss range of 0.5 eV from the quasielastic peak [see Fig. 2(b)], we expect to see low-energy excitations associated with the Kondo energy, crystal-field, and spin-orbit interactions. Our energy resolution ( $\approx 100$  meV) is not enough to resolve the crystal-field features ( $\sim 5$  and 12 meV for CeAgSb<sub>2</sub>) which contribute to the relatively broad quasielastic loss peak. The spin-orbit energy in Ce compounds is known to be  $280 \pm 10$  meV [8–11] and can be resolved with our energy resolution. Finally, the Kondo resonance is expected in the spectral function of the SIAM to be just above the Fermi level and corresponds to the energy ( $k_B T_K$ ) between the singlet Kondo ground state and the excited manifold of magnetic  $f^1$  states. In order to study these low-energy excitations, RIXS spectra were measured with an incident  $h\nu$  indicated by point B in the XAS spectrum shown in Fig. 1(a). Indeed, at this energy the intermediate states dominated by the  $3d^9 4f^2$  decay predominantly to states with  $f^1$  character, i.e., in an energy range close to the zero energy loss peak [see Fig. 2(a)]. As mentioned above, the hybridization between the  $f$  states and conduction band states lifts the degeneracy of the spin-orbit levels, and two singlet states  $|\Psi_0\rangle$  and  $|\Psi_2\rangle$  are stabilized [see Fig. 2(a)]. These two singlet states have zero total angular momentum, whereas the corresponding excited states  $|\Psi_1\rangle$  and  $|\Psi_3\rangle$  correspond to manifolds with  $f_{5/2}^1$  and  $f_{7/2}^1$  characters, respectively. Figure 2(b) shows the experimental and simulated RIXS spectra below 0.5 eV energy loss measured with  $\pi$  and  $\sigma$  polarizations for  $h\nu$  indicated by point B. In the  $\sigma$  polarization, two features separated by 280 meV (matching the spin-orbit energy) are observed with a dominant nearly zero energy peak. This behavior is satisfactorily reproduced by the calculation. The experimental peak near zero energy loss is composed of two unresolved contributions, one corresponding to the  $|\Psi_0\rangle$  final state and the second corresponding to the  $|\Psi_1\rangle$  manifold, which appears as a shoulder in the calculated spectrum. This is due to the fact that the singlet stabilization in our zero conduction bandwidth SIAM cannot provide the correct value of  $T_K$  (it is much larger than the known  $T_K$  for CeAgSb<sub>2</sub>, and then it leads to a shoulder feature at an overestimated energy). The second experimental structure appearing close to 280 meV is a spin-orbit replicate. It is also composed of two contributions corresponding to transitions to the singlet  $|\Psi_2\rangle$  state (with a very low spectral weight) and to the  $|\Psi_3\rangle$  manifold. As discussed above, in the  $\pi$  polarization, the transitions to final states with zero total angular momentum ( $|\Psi_0\rangle$  and  $|\Psi_2\rangle$ ) are forbidden. Thus, the spectrum exhibits only the two structures corresponding to the transitions to the  $|\Psi_1\rangle$  and  $|\Psi_3\rangle$  final states. The  $4f$  spin-orbit energy (280 meV) estimated from the separation energy of the two RIXS structures is in good agreement with high-resolution PES measurements (280 meV) [8–11,38].

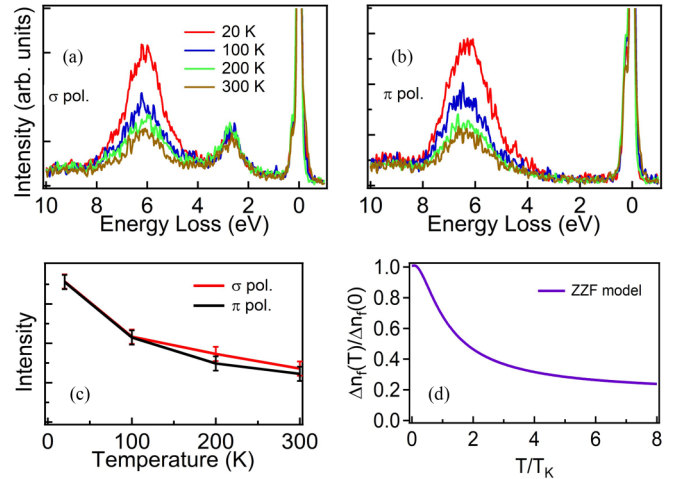


FIG. 3. Temperature dependence of the fluorescencelike structure in (a)  $\sigma$  and (b)  $\pi$  polarizations. The incident photon energy is tuned on the XAS satellite (spectrum G). (c) Evolution of the intensity fluorescencelike structure in  $\sigma$  and  $\pi$  polarization with temperature. (d) Temperature dependence of  $\Delta n_f(T)/\Delta n_f(0)$  calculated using the ZZF approach.

Similarly, the polarization dependence of the RIXS spectra with the incident  $h\nu$  equal to point G of the XAS satellite (associated with intermediate states with a  $f^1$  character) is clearly evidenced in Figs. 3(a) and 3(b). As theoretically predicted, the  $f^0$  final state is completely suppressed in the  $\pi$  polarization, and by disregarding the fluorescencelike structure, the spectra are similar to those of a purely trivalent compound. This behavior is nicely reproduced by the simulations [see Fig. 1(d)] and confirms the  $^1S_0$  symmetry of the initial state. This brings us to the remaining feature seen in the RIXS spectra, the fluorescence structure [vertical bars in Fig. 1(c)]. Normal fluorescence, which appears for the incident  $h\nu$  tuned well above the threshold, was observed at 17 and 22 eV and attributed to the  $5p \rightarrow 3d$  emission [50] and the MMN Coster-Kronig transition ( $3d_{5/2} \rightarrow 3d_{3/2}$  emission) [27]. The structure observed at 6 eV loss energy for  $h\nu$  at point G is attributed to a fluorescencelike structure to discriminate it from the normal fluorescence and has also been observed in CeB<sub>6</sub> [27] and CeO<sub>2</sub> [48] but not in CeF<sub>3</sub> [51]. Since it has the highest intensity at  $h\nu$  at point G, it is likely associated with the  $f^0$  character in the ground state. Kotani [52] proposed that in  $d^0$  compounds, such a fluorescencelike structure is associated with a mechanism in which an excited  $3d$  electron can escape to the neighboring site when incident  $h\nu$  is tuned on the XAS satellite  $f^0 \rightarrow f^1$  peak. Figures 3(a) and 3(b) show the  $T$  dependence of RIXS spectra with the incident  $h\nu$  tuned on the XAS satellite (point G). It is well known that the XAS satellite intensity exhibits a  $T$  dependence which follows a universal scaling behavior as a function of  $T/T_K$  like the Kondo resonance in IPES [3,13,53,54]. Indeed, the XAS spectra appear to be similar to those of purely trivalent compounds at high  $T \gg T_K$ , whereas at low  $T \ll T_K$  an additional structure is observed which reflects mixed-valence character [39]. Interestingly, the fluorescencelike structure exhibits a strong  $T$  dependence.

In the SIAM, the Kondo resonance and its spin-orbit replicas exhibit a temperature dependence reflecting the Kondo energy and the breakdown of the Kondo singlet state [3]. If the crystal-field interaction is included in the calculations, additional Kondo replicas appear at the energies of the excited crystal electric field (CEF) levels, and all of them exhibit the temperature dependence driven by the Kondo energy, as shown experimentally by Ehm *et al.* [10]. Core level photoemission and  $3d$  XAS spectra also reflect this Kondo energy. Indeed, as discussed above, the intensity of the XAS satellite structure reflects the degree of delocalization of the  $f$  states in the ground state, and no fluorescence-like structure is observed in the RIXS spectra of the purely trivalent  $\text{CeF}_3$  compound. Moreover, with increasing  $T$ , the purely trivalent first excited states located at  $k_B T_K$  are progressively populated, and no fluorescence is expected for these states, similar to the  $\text{CeF}_3$  ground state. A strong  $T$  dependence is actually observed in both  $\pi$  and  $\sigma$  polarizations [Fig. 3(c)], leading us to conjecture that this dependence could reflect the Kondo energy scale. This scenario is corroborated by a comparison with the calculation of the  $T$  dependence of the  $f^0$  weight in the ground state [ $\Delta n_f(T) = 1 - n_f(T)$ ]. We used the Zwicknagl, Zevin and Fulde (ZZF) approach [55,56], a well-established simplification of the noncrossing approximation in the SIAM including the crystal-field interaction. We performed the calculation with  $n_f(0) = 0.987$  and using a  $\Gamma_6$  ground state, with  $\Gamma_7^1$  and  $\Gamma_7^2$  crystal-field excited states at 5 and 12 meV, respectively, and the results suggest qualitative consistency with the  $T$ -dependent fluorescence intensity [Fig. 3(d)]. Nevertheless, a many-body description of the fluorescence structure in temperature-dependent simulations of RIXS spectra, for example, in the noncrossing approximation of the SIAM, is required to confirm the interplay of the Kondo energy scale and the fluorescence structure.

We propose a mechanism similar to the one proposed by Kotani for  $d^0$  systems recently assigned as an indirect RIXS process [57]. When the incident  $h\nu$  energy is tuned on the XAS  $f^0$  structure, which reflects an admixture of the  $4f$  states with the continuum, a conduction electron escapes to the  $4f$  state, leaving behind a hole in the conduction band.

The probability of this process  $3d^{10}4f^0 \rightarrow 3d^94f^1 \rightarrow 3d^94f^2 + \underline{\phantom{L}} \rightarrow 3d^{10}4f^1$  (with  $\underline{\phantom{L}}$  denoting a hole in the conduction band) increases with the hybridization strength between the  $f$  states and the conduction states. Therefore, the weight of the fluorescence structure would depend on the weight of the  $f^0$  configuration in the initial state. This is compatible with the fact that the RIXS spectrum of a purely trivalent compound like  $\text{CeF}_3$  does not exhibit such a fluorescence structure. Moreover, in a Kondo system with a contribution of the  $f^0$  configuration in the ground state, its intensity should be proportional to  $1 - n_f$ , and accordingly, its intensity should decrease with increasing temperature with a progressive breakdown of the Kondo singlet and the population of  $f^1$  states. This is in qualitative agreement with the observed behavior.

#### IV. CONCLUSIONS

We have shown that Ce  $M_5$  edge resonant inelastic x-ray scattering spectroscopy is a powerful technique to measure the spin and charge excitations in Ce-based Kondo systems. By tuning the incident photon energy around the main and XAS satellite structures, we have investigated the electronic structure of the  $\text{CeAgSb}_2$  Kondo system. We determined the  $f^1 \rightarrow f^2$  and  $f^1 \rightarrow f^0$  charge excitations as well as the spin-orbit excitation. We exploited the polarization dependence which allows the determination the symmetry of the ground state. All spin and charge excitations are well understood in the framework of the single-impurity Anderson model combined with the full multiplet theory. We also evidenced a strong  $T$  dependence of the fluorescence-like structure that we interpret as evidence of the Kondo energy scale.

#### ACKNOWLEDGMENTS

D.M. and A.C. thank the France-Taiwan (CNRS-MOST) bilateral project for financially supporting this research under Contracts No. CNRS 290771 and No. MOST 109-2911-I-213-501. A.C. thanks the National Science and Technology Council of Taiwan for financially supporting this research under Contract No. MOST 108-2112-M-213-001-MY3.

- 
- [1] A. C. Hewson, *The Kondo Problem to Heavy Fermions* (Cambridge University Press, Cambridge, 1993).
  - [2] P. Coleman, Heavy Fermions: Electrons at the edge of magnetism, in *Handbook of Magnetism and Advanced Magnetic Materials*, edited by H. Kronmüller, S. Parkin, and I. Zutic (John Wiley and Sons, 2007), Vol. 1, pp. 95–148.
  - [3] N. E. Bickers, D. L. Cox, and J. W. Wilkins, *Phys. Rev. B* **36**, 2036 (1987); N. E. Bickers, *Rev. Mod. Phys.* **59**, 845 (1987).
  - [4] O. Gunnarsson and K. Schönhammer, *Phys. Rev. B* **28**, 4315 (1983).
  - [5] J. C. Fuggle, F. U. Hillebrecht, Z. Sołnierek, R. Lässer, C. Freiburg, O. Gunnarsson, and K. Schönhammer, *Phys. Rev. B* **27**, 7330 (1983).
  - [6] J. W. Allen, S. J. Oh, O. Gunnarsson, K. Schönhammer, M. B. Maple, M. S. Torikachvili, and I. Lindau, *Adv. Phys.* **35**, 275 (1986).
  - [7] G. Poelchen, S. Schulz, M. Mende, M. Güttler, A. Generalov, A. V. Fedorov, N. Caroca-Canales, C. Geibel, K. Kliemt, C. Krellner, S. Danzenbächer, D. Yu. Usachov, P. Dudin, V. N. Antonov, J. W. Allen, C. Laubschat, K. Kummer, Y. Kucherenko, and D.V. Vyalikh, *npj Quantum Mater.* **5**, 70 (2020).
  - [8] D. Malterre, M. Grioni, and Y. Baer, *Adv. Phys.* **45**, 299 (1996).
  - [9] F. Reinert, D. Ehm, S. Schmidt, G. Nicolay, S. Hüfner, J. Kroha, O. Trovarelli, and C. Geibel, *Phys. Rev. Lett.* **87**, 106401 (2001).
  - [10] D. Ehm, S. Hüfner, F. Reinert, J. Kroha, P. Wölfle, O. Stockert, C. Geibel, and H. v. Löhneysen, *Phys. Rev. B* **76**, 045117 (2007).
  - [11] S. Patil, A. Generalov, M. Güttler, P. Kushwaha, A. Chikina, K. Kummer, T. C. Rödel, A. F. Santander-Syro, N. Caroca-Canales, C. Geibel, S. Danzenbächer, Yu. Kucherenko,

- C. Laubschat, J. W. Allen, and D. V. Vyalikh, *Nat. Commun.* **7**, 11029 (2016).
- [12] F. U. Hillebrecht, J. C. Fuggle, G. A. Sawatzky, M. Campagna, O. Gunnarsson, and K. Schönhammer, *Phys. Rev. B* **30**, 1777 (1984).
- [13] D. Malterre, M. Grioni, P. Weibel, B. Dardel, and Y. Baer, *Phys. Rev. Lett.* **68**, 2656 (1992).
- [14] D. Malterre, M. Grioni, P. Weibel, B. Dardel, and Y. Baer, *Europhys. Lett.* **20**, 445 (1992).
- [15] M. Grioni, P. Weibel, D. Malterre, Y. Baer, and L. Du'ò, *Phys. Rev. B* **55**, 2056 (1997).
- [16] X. Wang, H. Michor, and M. Grioni, *Phys. Rev. B* **75**, 035127 (2007).
- [17] S. Banik, A. Arya, A. Bendounan, M. Maniraj, Thamizhavel, I. Vobornik, S. K. Dhar, and S. K. Deb, *J. Phys.: Condens. Matter* **26**, 335502 (2014).
- [18] J. C. Fuggle, F. U. Hillebrecht, J.-M. Esteva, R. C. Karnatak, O. Gunnarsson, and K. Schönhammer, *Phys. Rev. B* **27**, 4637 (1983).
- [19] K. Kanai, Y. Tezuka, T. Terashima, Y. Muro, M. Ishikawa, T. Uozumi, A. Kotani, G. Schmerber, J. P. Kappler, J. C. Parlebas, and S. Shin, *Phys. Rev. B* **60**, 5244 (1999).
- [20] T. Uozumi, K. Kanai, S. Shin, A. Kotani, G. Schmerber, J. P. Kappler, and J. C. Parlebas, *Phys. Rev. B* **65**, 045105 (2002).
- [21] L. J. P. Ament, M. van Veenendaal, T. P. Devereaux, J. P. Hill, and J. van den Brink, *Rev. Mod. Phys.* **83**, 705 (2011).
- [22] A. Kotani and S. Shin, *Rev. Mod. Phys.* **73**, 203 (2001).
- [23] A. Kotani, *Phys. Rev. B* **83**, 165126 (2011).
- [24] S. M. Butorin, D. C. Mancini, J.-H. Guo, N. Wassdahl, J. Nordgren, M. Nakazawa, S. Tanaka, T. Uozumi, A. Kotani, Y. Ma, K. E. Myano, B. A. Karlin, and D. K. Shuh, *Phys. Rev. Lett.* **77**, 574 (1996).
- [25] S. M. Butorin, M. Magnuson, K. Ivanov, D. K. Shuh, T. Takahashi, S. Kunii, J.-H. Guo, and J. Nordgren, *J. Electron Spectrosc. Relat. Phenom.* **101–103**, 783 (1999).
- [26] M. Nakazawa, S. Tanaka, T. Uozumi, and A. Kotani, *J. Phys. Soc. Jpn.* **65**, 2303 (1996).
- [27] M. Magnuson, S. M. Butorin, J.-H. Guo, A. Agui, J. Nordgren, H. Ogasawara, A. Kotani, T. Takahashi, and S. Kunii, *Phys. Rev. B* **63**, 075101 (2001).
- [28] C. Dallera, M. Grioni, A. Palenzona, M. Taguchi, E. Annesse, G. Ghiringhelli, A. Tagliaferri, N. B. Brookes, T. Neisius, and L. Braicovich, *Phys. Rev. B* **70**, 085112 (2004).
- [29] A. Amorese, G. Dellea, M. Fanciulli, S. Seiro, C. Geibel, C. Krellner, I. P. Makarova, L. Braicovich, G. Ghiringhelli, D. V. Vyalikh, N. B. Brookes, and K. Kummer, *Phys. Rev. B* **93**, 165134 (2016).
- [30] A. Amorese, N. Caroca-Canales, S. Seiro, C. Krellner, G. Ghiringhelli, N. B. Brookes, D. V. Vyalikh, C. Geibel, and K. Kummer, *Phys. Rev. B* **97**, 245130 (2018).
- [31] A. Amorese, K. Kummer, N. B. Brookes, O. Stockert, D. T. Adroja, A. M. Strydom, A. Sidorenko, H. Winkler, D. A. Zocco, A. Prokofiev, S. Paschen, M. W. Haverkort, L. H. Tjeng, and A. Severing, *Phys. Rev. B* **98**, 081116(R) (2018).
- [32] A. Amorese, D. Khalyavin, K. Kummer, N. B. Brookes, C. Ritter, O. Zaharko, C. B. Larsen, O. Pavlosiuk, A. P. Pikul, D. Kaczorowski, M. Gutmann, A. T. Boothroyd, A. Severing, and D. T. Adroja, *Phys. Rev. B* **105**, 125119 (2022).
- [33] E. Jobiliong, J. S. Brooks, E. S. Choi, H. Lee, and Z. Fisk, *Phys. Rev. B* **72**, 104428 (2005).
- [34] S. Araki, N. Metoki, A. Galatanu, E. Yamamoto, A. Thamizhavel, and Y. Ōnuki, *Phys. Rev. B* **68**, 024408 (2003).
- [35] J. A. Dann, A. D. Hillier, J. G. M. Armitage, and R. Cywinski, *Phys. B (Amsterdam, Neth.)* **289–290**, 38 (2000).
- [36] T. Takeuchi, A. Thamizhavel, T. Okubo, M. Yamada, N. Nakamura, T. Yamamoto, Y. Inada, K. Sugiyama, A. Galatanu, E. Yamamoto, K. Kindo, T. Ebihara, and Y. Ōnuki, *Phys. Rev. B* **67**, 064403 (2003).
- [37] D. Hafner, Binod K. Rai, J. Banda, K. Kliemt, C. Krellner, J. Sichelschmidt, E. Morosan, C. Geibel, and M. Brando, *Phys. Rev. B* **99**, 201109(R) (2019).
- [38] Y. Saitoh, H. Fujiwara, T. Yamaguchi, Y. Nakatani, T. Mori, H. Fuchimoto, T. Kiss, A. Yasui, J. Miyawaki, S. Imada, H. Yamagami, T. Ebihara, and A. J. Sekiyama, *J. Phys. Soc. Jpn.* **85**, 114713 (2016).
- [39] C. W. Chuang, B. Tegomo Chiogo, D. Malterre, P.-Y. Chuang, C.-M. Cheng, T.-W. Pi, F.-H. Chang, H.-J. Lin, C.-T. Chen, C.-N. Kuo, C.-S. Lue, and A. Chainani, *Electron. Struct.* **3**, 034001 (2021).
- [40] J. M. Imer and E. Wuilloud, *Z. Phys. B: Condens. Matter* **66**, 153 (1987).
- [41] M. W. Haverkort, M. Zwierzycki, and O. K. Andersen, *Phys. Rev. B* **85**, 165113 (2012).
- [42] M. W. Haverkort, *J. Phys.: Conf. Ser.* **712**, 012001 (2016).
- [43] M. Nakazawa, H. Ogasawara, and A. Kotani, *J. Phys. Soc. Jpn.* **69**, 4071 (2000).
- [44] C. H. Lai, H. S. Hung, W. B. Wu, H. Y. Huang, H. W. Fu, S. W. Lin, S. W. Huang, C. C. Chiu, D. J. Wang, L. J. Huang, T. C. Tseng, S. C. Chuang, C. T. Chen, and D. J. Huang, *J. Synchrotron Radiat.* **21**, 325 (2014).
- [45] See Supplemental Material at <http://link.aps.org/supplemental/10.1103/PhysRevB.106.075141> for (i) the experimental geometry of the RIXS measurements, (ii) details on the calculation method, (iii) a discussion of the importance of the  $f^2$  configuration in the ground state, and (iv) the temperature dependence of the RIXS spectra with  $\sigma$  polarization.
- [46] T. Willers *et al.*, *Phys. Rev. B* **85**, 035117 (2012).
- [47] M. Sundermann *et al.*, *J. Electron. Spectrosc. Relat. Phenom.* **209**, 1 (2016).
- [48] M. Watanabe, Y. Harada, M. Nakazawa, Y. Ishiwata, R. Euguchi, T. Takeuchi, A. Kotani, and S. Shin, *Surf. Rev. Lett.* **09**, 983 (2002).
- [49] N. Sasabe, H. Tonai, and T. Uozumi, *J. Phys. Soc. Jpn.* **86**, 093701 (2017).
- [50] C. Dallera, K. Giarda, G. Ghiringhelli, A. Tagliaferri, L. Braicovich, and N. B. Brookes, *Phys. Rev. B* **64**, 153104 (2001).
- [51] S. M. Butorin, D. C. Mancini, J.-H. Guo, N. Wassdahl, and J. Nordgren, *J. Alloys Compd.* **225**, 230 (1995).
- [52] T. Ide and A. Kotani, *J. Phys. Soc. Jpn.* **69**, 1895 (2000).
- [53] A. Delobbe, M. Finazzi, B. Buschinger, O. Trovarelli, Ch. Geibel, J.-P. Kappler, and G. Krill, *Phys. B (Amsterdam, Neth.)* **259–261**, 1144 (1999).
- [54] A. Amorese, A. Marino, M. Sundermann, K. Chen, Z. Hu, T. Willers, F. Choueikani, P. Ohresser, J. Herrero-Martin,

- S. Agrestini, C-Te. Chen, H. J. Lin, M. W. Haverkort, S. Seiro, C. Geibel, F. Steglich, L. H. Tjeng, G. Zwicknagl, and A. Severing, *Phys. Rev. B* **102**, 245146 (2020).
- [55] G. Zwicknagl, V. Zevin, and P. Fulde, *Z. Phys. B: Condens. Matter* **79**, 365 (1990).
- [56] V. Zevin, G. Zwicknagl, and P. Fulde, *Phys. Rev. Lett.* **60**, 2331 (1988).
- [57] K. Gilmore, J. Pelliciari, Y. Huang, J. J. Kas, M. Dantz, V. N. Strocov, S. Kasahara, Y. Matsuda, T. Das, T. Shibauchi, and T. Schmitt, *Phys. Rev. X* **11**, 031013 (2021).